Crystallization Behavior of Isotactic Propylene-1-Hexene Random Copolymer Revealed by Time-Resolved SAXS/WAXD Techniques

YIMIN MAO,[1] FENG ZUO,[1] JONG KAHK KEUM,[1] BENJAMIN S. HSIAO,[1] DEREK W. THURMAN,[2] ANDY H. TSOU[3]

[1]Department of Chemistry, Stony Brook University, Stony Brook, New York 11794-3400

[2]ExxonMobil Chemical Company, 5200 Bayway Drive, Baytown, Texas 77520

[3]ExxonMobil Research and Engineering Company, Annandale, New Jersey 08801

Received 12 May 2009; revised 24 August 2009; accepted 31 August 2009
DOI: 10.1002/polb.21840
Published online in Wiley InterScience (www.interscience.wiley.com).

ABSTRACT: The crystallization behavior of isotactic propylene-1-hexene (PH) random copolymer having 5.7% mole fraction of hexene content was investigated using simultaneous time-resolved small-angle X-ray scattering (SAXS) and wide-angle X-ray diffraction (WAXD) techniques. For this copolymer, the hexene component cannot be incorporated into the unit cell structure of isotactic polypropylene (iPP). Only α-phase crystal form of iPP was observed when samples were melt crystallized at temperatures of 40 °C, 60 °C, 80 °C, and 100 °C. Comprehensive analysis of SAXS and WAXD profiles indicated that the crystalline morphology is correlated with crystallization temperature. At high temperatures (e.g., 100 °C) the dominant morphology is the lamellar structure; while at low temperatures (e.g., 40 °C) only highly disordered small crystal blocks can be formed. These morphologies are kinetically controlled. Under a small degree of supercooling (the corresponding iPP crystallization rate is slow), a segmental segregation between iPP and hexene components probably takes place, leading to the formation of iPP lamellar crystals with a higher degree of order. In contrast, under a large degree of supercooling (the corresponding iPP crystallization rate is fast), defective small crystal blocks are favored due to the large thermodynamic driving force and low chain mobility. J Polym Sci Part B: Polym Phys 48: 26–32, 2010

KEYWORDS: crystallization; morphology; propylene-1-hexene; random copolymer; SAXS; WAXD

INTRODUCTION Random copolymer is synthesized via copolymerization of two or more monomers of different chemical compositions, in which a statistically distributed structure along the chain backbone is obtained. If there are repulsive interactions among different species of the segments (this can be quantified using Flory's interaction parameter, χ), hierarchical textures can be formed through micro-phase separation taking place at different length scale.[1–4] Thus, one can control the morphology of random copolymer by adjusting the composition parameters such as the comonomer ratio and sequence distribution.[2,5,6] If one of the components in the copolymer is crystallizable, the structure formation can become complicated since two types of demixing processes can be involved, that is, micro-phase separation among the segments of different species and liquid-solid (L-S) phase transformation between the crystalline and amorphous phases.[7,8] The interplay between the two processes controls the final morphology.

From the crystallization standpoint, random copolymer differs from homopolymer in two main aspects. First, by introducing noncrystallizable components randomly into crystallizable backbone, the chain regularity as well as the ability of chain sliding are decreased, which would lead to low crystallinity. Second, the sequence length of the crystallizable component in random copolymer also decreases, which would lead to shorter lamellar thickness. As a result, crystalline in random copolymers always shows a lower melting temperature and broader enthalpy change in differential scanning calorimetry (DSC) measurement as compared with those of homopolymers.[7,9–11] These features make the properties of crystallizable random copolymers very different from homopolymers, and thus provide considerable commercial potential.[12,13]

In this study, we have investigated the crystallization behavior of propylene-1-hexene (PH) random copolymer using time-resolved small-angle X-ray scattering (SAXS) and wide-angle X-ray diffraction (WAXD) techniques. The *in situ* SAXS/WAXD results have provided insightful information about structure formation in a length scale ranging from several angstroms (i.e., crystal unit cell) to several hundreds of nanometers (i.e., crystal morphology). The relationship of crystal morphology and crystallization kinetics under

Correspondence to: B. S. Hsiao (E-mail: bhsiao@notes.cc.sunysb.edu)

different crystallization temperatures could be correlated. The results of this random copolymer may be quite universal to other random copolymers containing different types of olefin components.

EXPERIMENTAL

Materials and Experimental Procedures

The chosen PH random copolymer was synthesized by the ExxonMobil Chemical Company. The number average molecular weight (M_n) of the chosen sample was 14,300 g/mol and the polydispersity was 2.8. The mole fraction of the hexene component was 5.7%. The sample showed a broad melting peak ranging from 123.7 to 134.7 °C, with a peak position located at 126.4 °C in DSC trace (with 10 °C/min heating rate).

The temperature protocol for the synchrotron X-ray experiment is as follows. The sample was first melted at 200 °C for 5 min to remove all residual stress and thermal history. After that, the sample was quenched (at a cooling rate of −100 °C/min) to desired temperatures for the isothermal crystallization experiment. An INSTECH hot stage equipped with a precision temperature controller was used to heat treat the samples, where the accuracy of the temperature control was ±0.1 °C. The isothermal crystallization process was monitored *in situ* by time-resolved SAXS/WAXD techniques, which will be described next. Four temperatures, 40 °C, 60 °C, 80 °C, and 100 °C, were chosen for the study.

Combined SAXS/WAXD Measurements

Combined SAXS/WAXD measurements were carried out at the Advanced Polymer Beamline (X27C) in the National Synchrotron Light Source (NSLS), Brookhaven National Laboratory (BNL). The wavelength of the X-ray beam was 1.371 Å. All scattering and diffraction images were captured *in situ* by 2D MAR CCD detector, where the exposure time for each image collection was 30 seconds. The sample-to-detector distances were 1890.0 mm for SAXS measurement and 120.6 mm for WAXD measurement. The SAXS and WAXD measurements were carried out separately with the same sample and temperature protocol. The scattering angle of the SAXS patterns was calibrated with silver behenate ($AgC_{22}H_{43}O_2$) and the diffraction angle of the WAXD signals was calibrated by Al_2O_3. All images were corrected for beam fluctuations and background scattering in the data analysis.

RESULTS AND DISCUSSION

The crystal structure of isotactic PH random copolymer can be determined by the WAXD method. Figure 1 shows integrated intensity profiles from the final 2D WAXD patterns of PH copolymer fully crystallized under 100 °C, 80 °C, 60 °C, and 40 °C, respectively. In these profiles, the integrated diffraction intensity is plotted against the absolute value of scattering vector s ($s = \frac{2}{\lambda}\sin\frac{\theta}{2}$, where λ represents the wavelength and θ is the diffraction angle). Although varied in magnitude, all profiles in Figure 1 exhibit four diffraction peaks located at the s values of 1.57, 1.87, 2.06, and 2.41 nm^{-1}. These peaks match the characteristic reflections

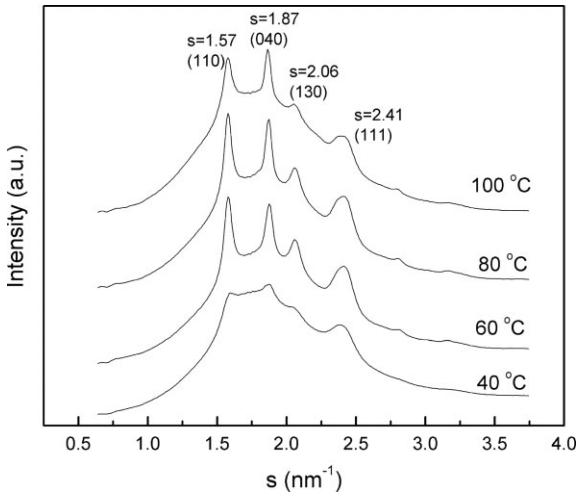

FIGURE 1 Final integrated WAXD profiles of PH copolymer fully melt crystallized at 100 °C, 80 °C, 60 °C, and 40 °C.

from the α-phase crystal form of i-PP homopolymer[14] and they can be indexed as 110, 040, 130, and 111 reflections, respectively. Earlier studies indicated that in PH random copolymer, the hexene moiety can be incorporated into the crystal structure and form new crystal forms, different from the known α, β and γ forms of i-PP homopolymer, when the hexene content is sufficiently high.[15–17] For example, de Rosa et al.[16] reported that when the hexene content was above 10 mol %, a new crystal form with trigonal unit cell structure became favorable, containing a threefold propylene-hexene copolymer unit with *R*3*c* or $R\bar{3}c$ space group. In our case, no new crystal form was observed under the chosen crystallization conditions probably due to the low content of hexene inclusion (5.7% mole fraction).

To investigate the crystallization kinetics, the evolutions of crystallinity as a function of time at different temperatures are shown in Figure 2(a). The degree of crystallinity was estimated from the integrated WAXD profile, by dividing the sum of the areas under all crystalline peaks by that of the total area (this procedure was carried out by deconvoluting the diffraction profile into crystalline and amorphous components using a curve fitting program). The "crystallinity" obtained in this way should be termed as crystallinity index, for it is not truly equivalent to the absolute value of crystallinity. Hereafter, such "crystallinity" will be used to show the general trend of the crystallization process in this study. In Figure 2(a). the crystallinity curve of sample isothermally crystallized at 100 °C shows a typical behavior, containing three stages: an early stage that can be called the induction period where crystallinity equals zero; an intermediate stage where crystallinity increases with time; and a late stage where crystallinity reaches a plateau value, indicating crystallization is fully accomplished. As the crystallization temperature decreases, the crystallization kinetics becomes faster. This can be clearly seen from Figure 2(b) which

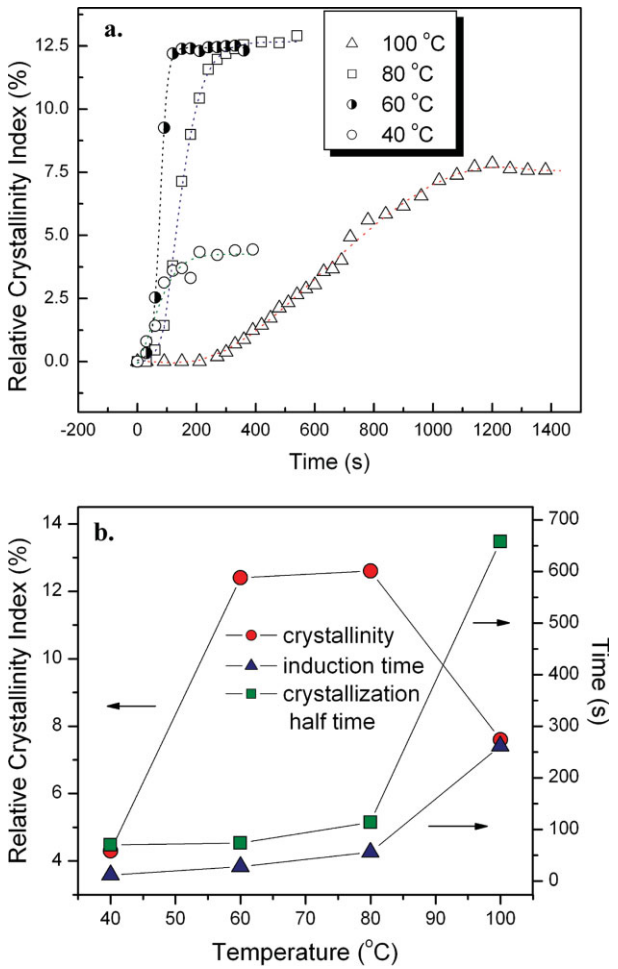

FIGURE 2 (a) Crystallinity versus time plots of samples crystallized at 100 °C, 80 °C, 60 °C, and 40 °C. (b) Induction time and crystallization half time obtained from each curve in (a) at different temperatures. [Color figure can be viewed in the online issue, which is available at www.interscience.wiley.com.]

displays induction time and crystallization half time obtained from Figure 2(a) at different temperatures. Both parameters increase (i.e., the slower crystallization rate) with crystallization temperature. In Figure 2(b), the induction time was determined by extrapolating the interception between the early stage and intermediate stage, where the crystallization half time is the time span that the sample requires to achieve half of its final crystallinity. The highest crystallinity achieved in the chosen sample was around 12% when samples were annealed at temperatures of 60 and 80 °C. This might be due to the optimal coupling of chain mobility and the crystallization driving force (i.e., degree of supercooling). However, this crystallinity value is very low when compared with that typically found in fully crystallized i-PP homopolymer (>60%). This is because the non-crystallizable hexene component has significantly hindered the crystallization ability of random copolymer, which will be discussed later.

The crystallization curves from samples crystallized at temperatures of two opposite ends, that is, 100 °C and 40 °C, are quite different and deserve a close examination. The difference in kinetics appears to be associated with the different crystalline structure. Figure 3 shows the evolution of SAXS profiles for PH copolymer annealed at (a) 100 °C and (b) 40 °C, respectively. It is seen that SAXS profiles at 100 °C [Fig. 3(a)] gradually exhibit a scattering maximum, corresponding to a long period of about 18 nm. The corresponding WAXD reflections also become intense and sharp. These are classic features of the lamellar crystalline structure. In contrast, SAXS profiles at 40 °C are featureless [Fig. 3(b)], whereby the scattering intensity decreases monotonically with *s*. The lack of the scattering maximum in the SAXS profiles at 40 °C indicates that the scatterers formed under this condition have little or no correlation with each other. Nevertheless, the corresponding WAXD profile in Figure 1 still exhibits four identifiable diffraction peaks, though weak and diffuse compared with those at 100 °C, indicating the existence of crystal structure. The estimated crystallinity under this condition is only about 5% (Fig. 2). The above results indicate that the morphology of the PH sample annealed at

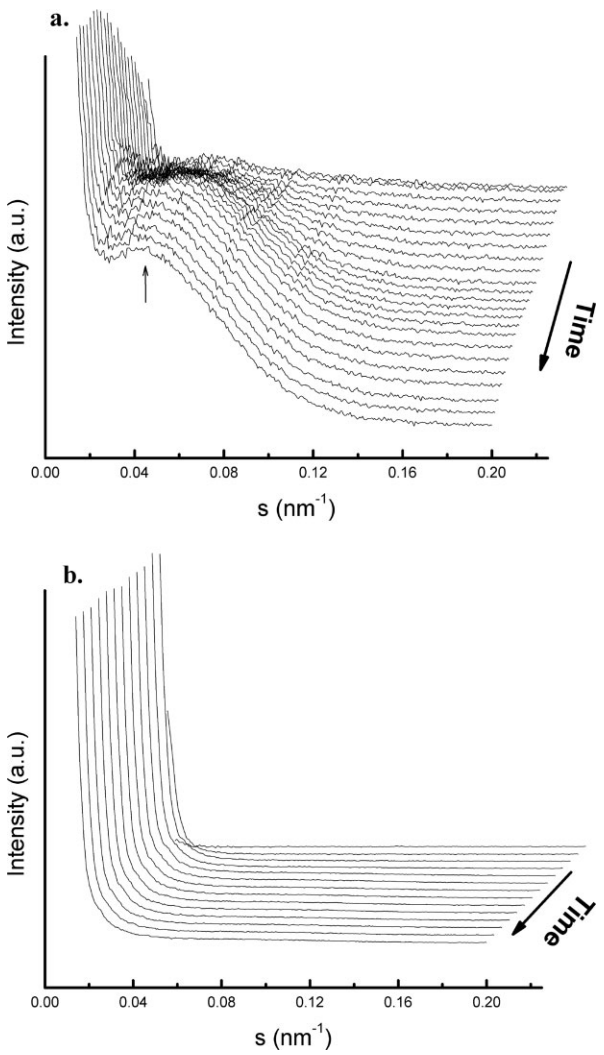

FIGURE 3 Evolutions of SAXS profiles for samples crystallized at (a) 100 °C and (b) 40 °C.

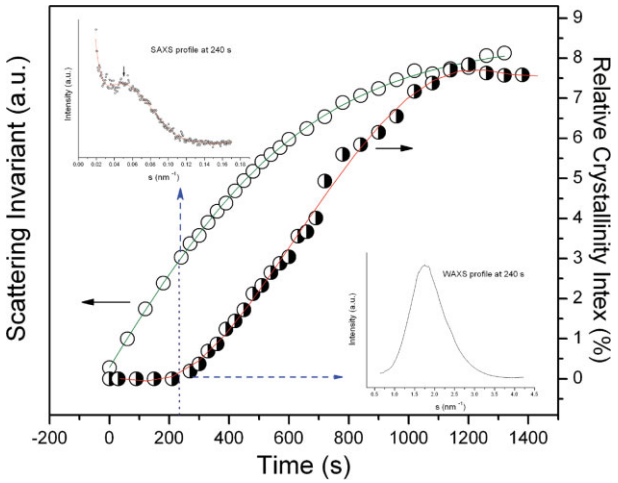

FIGURE 4 Scattering invariant (left) and relative crystallinity index (right) versus time plot when sample was melt crystallized at 100 °C. The two insets exhibit SAXS and WAXD profiles at 240s, which is in the end of the induction period. [Color figure can be viewed in the online issue, which is available at www.interscience.wiley.com.]

40 °C probably consists of sparsely dispersed small blocks of crystals with a large amount of defects imbedded.

Figure 4 represents the comparison of scattering invariant (left y-axis) and crystallinity (right y-axis) changes as a function of time when samples were crystallized at 100 °C. The scattering invariant Q was obtained from the SAXS profile using the following expression.[18]

$$Q = \int_0^\infty I(q)q^2dq \qquad (1)$$

The value of Q is proportional to the mean square density fluctuations occurring in the system, where the fluctuations include all phase changes leading to the inhomogenity of the system (e.g., both crystallization and micro-phase separation will contribute to the invariant). In Figure 4, it is seen that at the crystallization temperature of 100 °C, PH copolymer experiences an induction period of about 240 s, within which no signal change in WAXD can be detected. However, during this period, the SAXS scattering invariant continues to rise; and the SAXS profiles at the end of the induction period actually exhibit a broad shoulder indicating the existence of a weak correlation of the formed texture. However, this texture may not contain crystalline structure since no reflection peaks in WAXD were detected in the mean time. The physical origin of the increase of scattering invariant before crystallization might be quite complicated. Our previous study indicated that even for i-PP homopolymer, the crystallization onset time determined from the SAXS method appeared earlier than that from the WAXD method.[19] In homopolymer, the density fluctuations can be a driving force for the formation of a precursor structure that subsequently triggers further crystallization. Similar results have also been reported by other authors using different characterization techniques, such as polarized light scattering and rheological measurement.[20–22] For the random copolymer, the factor of phase segregation between two incompatible species should also be considered to explain the SAXS signal at an early stage. The micro-phase separation behavior in random copolymer has been well predicted by several theoretical works[2,5,6,23] and computer simulations[24–26]; and it has also been experimentally verified.[27,28] In this study, the hexene comonomer cannot be incorporated into crystal structure; the density fluctuation during the induction period could be a hybridization of both processes, followed by subsequent crystallization. To take a close look, the time-resolved SAXS profiles [Fig. 3(a)] are divided into two parts, as shown in Figure 5(a,b). In Figure 5, all symbols represent the corrected scattering data points and the solid lines represent the corresponding polynomial fitted curves. In the early stage [Fig. 5(a)], the scattering profiles are generally weak, but they do persistently exhibit a scattering peak (the first profile showing the scattering peak is at $t > 90$ s) at a fixed

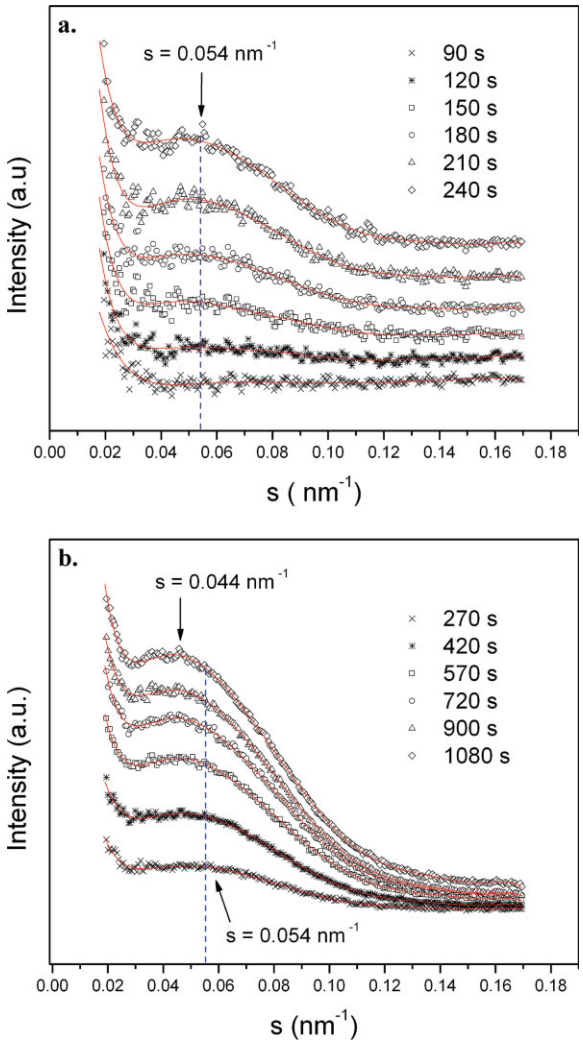

FIGURE 5 Time-resolved SAXS profiles during crystallization at 100 °C (a) during the induction period, (b) after the induction period. [Color figure can be viewed in the online issue, which is available at www.interscience.wiley.com.]

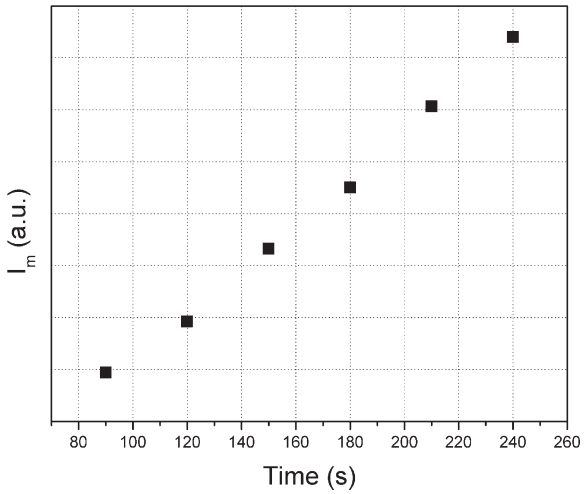

FIGURE 6 Change of peak intensity as a function of time during the early stage of crystallization at 100 °C.

location ($s = 0.054$ nm^{-1}), which corresponds to a long period of $L = 1/s = 18.5$ nm. After the induction period, crystallization took place and the lamellar crystalline structure was subsequently formed. Figure 5(b) shows the evolution of SAXS profile during this period. It is found that the intensity maximum is shifted toward a lower angle as crystallization proceeds and is eventually fixed at s = 0.044 nm^{-1}. In homopolymer, once the general shape of lamellar structure is formed, the position of the SAXS maximum usually remains unchanged in the early stage of the annealing. In the late stage, very often, the scattering maximum can move to a larger angle due to the interpenetration of new lamellae induced by secondary crystallization. Thus, shifting of the scattering maximum toward a lower angle, as observed in our experiment, is probably caused by the continuous exclusion of hexene segments from the crystalline structure, leading to an increase of long period. This should not be surprising as the large hexene moiety may not be incorporated into the crystal structure in our specimen. For this reason, we believe that the segregation between hexene and propylene segments may be the dominant factor responsible for the increase of scattering invariant in the early stage. Furthermore, this segregation process may play an important role in subsequent development of crystalline structure, that is, long annealing would favor the development of conventional lamellar structure, whereas rapid quenching would lead to disordered small crystal blocks.

In Figure 5(a), the peak position remains unchanged in the induction period, but its magnitude increases with time, which is shown in Figure 6. Generally there are two mechanisms for phase separation, that is spinodal decomposition (SD) and nucleation and growth (NG). In our study, it is difficult to conclude which one better fit the segregation process because the scattering intensity in the early stage is too weak for detailed analysis. In Figure 6, it is hard to judge whether the relationship of peak intensity and time can be described by exponential or power function. Trustworthy analysis of the early stage density fluctuation process must rely on a well-chosen model system, which should give good phase contrast between segregated domains. Furthermore, crystallization temperature must be carefully chosen so that the induction time is long enough to generate sufficient data points. At the final stage of crystallization, the peak fixates at the position of $s = 0.044$ nm^{-1}, corresponding to the long period of 22.7 nm. The lamellar thickness can be estimated via the ideal two-phase model. In this case, the long period represents the total length of the periodicity with combined crystalline and amorphous layers. For this purpose, the lamellar thickness was calculated by multiplying the long period with the crystalline fraction (i.e., 7.8% as shown in Fig. 3), which resulted in a value of 17.7 Å. Even though the two-phase model may underestimate the lamellar thickness because of the possible existence of the transition layer, this value is still very small as compared with the typical lamellar thickness for i-PP homopolymer (~100 Å). Some recent studies for random ethylene-based copolymer system[7,9–11,29] reported the existence of thin lamellar structure because of the lower melting temperature, which is consistent with our findings. These results are different from Flory's model,[30] which prohibits chain folding in random copolymer.

Figure 7 illustrates the comparison of the crystallinity (from WAXD) and invariant (from SAXS) for crystallization at 40 °C. Under this condition, due to the large degree of supercooling, the crystallization kinetics are greatly enhanced. It is seen that both scattering invariant and crystallinity increase with time in a similar trend. The diffraction peaks are observed in the very early stage of crystallization, where the pattern remains unchanged after 200 s. The insets in Figure 7 show the integrated profiles of SAXS and WAXD when crystallization was completed. The reflection peaks in WAXD are very weak and diffuse, where their positions can be indexed to the α-form crystal (Fig. 1). The monotonically decreased SAXS profile indicates that the system consists of

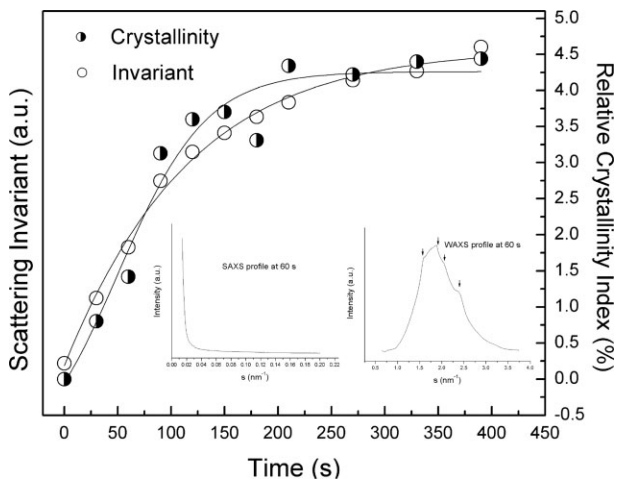

FIGURE 7 Scattering invariant (left) and relative crystallinity index (right) versus time plot when sample was crystallized at 40 °C. The two insets exhibit SAXS and WAXD profiles at the very beginning of the crystallization process.

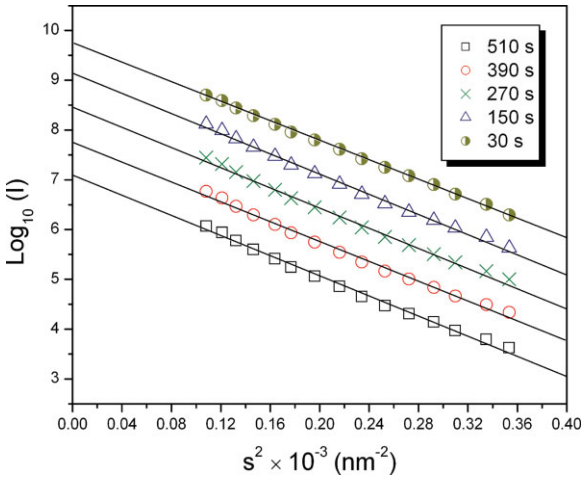

FIGURE 8 Guinier plots obtained from SAXS profiles of sample crystallized at 40 °C.

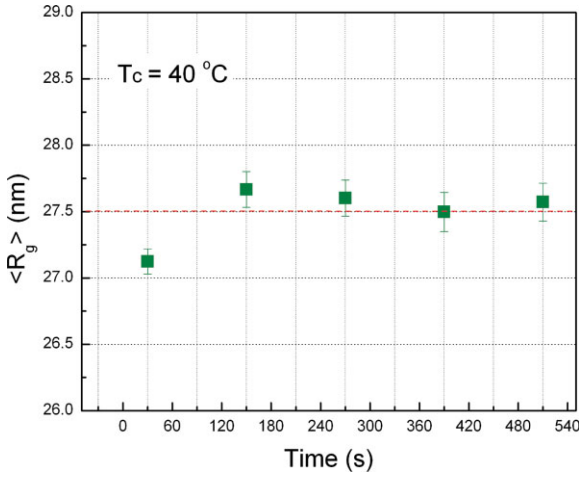

FIGURE 9 Radius of gyration (obtained from Guinier's plot) change as a function of time (crystallization temperature was 40 °C).

uncorrelated crystal blocks that are probably small and defective. Dimension of the crystal block can be estimated by using the Guinier's method[31–33] which correlates the scattering intensity and radius gyration of aggregate in dilute solution at low angles, as expressed in eq 2,

$$I_s = I_0 \exp\left(-\frac{R_g^2 q^2}{3}\right) \tag{2}$$

where I_s is the scattering intensity and I_0 is intensity of incident light. R_g is the radius of gyration, q is the wave vector which has the same physical meaning as s ($q = 2\pi s$). By applying logarithmic operation on both sides, eq 2 can be rewritten as

$$\ln(I_s) = \ln I_0 - \frac{R_g^2}{3} q^2 \tag{3}$$

Plotting $\ln(I_s)$ against q^2 or s^2 leads to a straight line and the radius of gyration can be obtained from its slope. Figure 8 shows a series of Guinier plots obtained at different times and crystallization temperature of 40 °C based on eq 3. The radius of gyration calculated from all the Guinier plots is around 27.5 nm, which remains almost unchanged during crystallization (as shown in Fig. 9). The dimension of small crystal block at 40 °C and that of lamellar crystalline structure at 100 °C are in the same order of magnitude. At this temperature, crystal blocks were quickly developed into this dimension due to a large driving force. The rapidly-formed crystals could hardly grow further and perfect their structure because of the low chain mobility. These blocks are highly disordered and therefore not stable, which can be seen by comparing the melting behavior of both crystallites formed at 40 °C and 100 °C. This experiment was carried out by gradually melting (4 °C/min) the fully crystallized sample after isothermal crystallization. The changes of crystallinity derived by *in situ* WAXD experiments under both conditions are illustrated in Figure 10. The hollow circles represent the crystallinity change during heating of the sample fully crystallized at 40 °C. The initial crystallinity, as was shown earlier, is 4.8% and it remains unchanged until at a temperature of around 60 °C, indicating that the chains at these low temperatures are still not sufficiently mobile. From 60 to 100 °C the crystallinity increases notably due to recrystallization process. After this period, the crystallinity begins to decrease until the sample becomes completely molten. The heating process of sample crystallized at 100 °C is displayed as hollow squares, where the crystallinity increases very slightly then begins to decrease with the increasing temperature. Above 118.2 °C (point **c**), the crystallinity of samples crystallized at two different temperatures merges into the same trend, as represented by the solid line. The extrapolated nominal melting point in Figure 10 is 140 °C. By intercepting the solid line with the initial stage of melting (i.e., the horizontal dotted line), melting point for samples crystallized at different temperatures can be

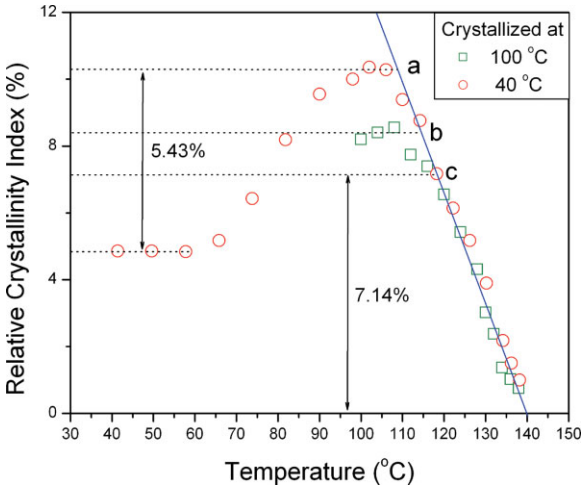

FIGURE 10 The crystallinity change during heating (at a heating rate of 4 °C/min) of samples fully crystallized at 100 °C (□) and at 40 °C (○).

determined: melting point **a** at 108.4 °C for the sample crystallized at 40 °C, and melting point **b** at 114.8 °C for the sample crystallized at 100 °C. The difference of 6.4 °C indicates the less stable crystalline structure formed at the lower crystallization temperature, which is consistent with the results from the structure analysis made earlier. In Figure 10, the crystallinity change from point **c** to zero is 7.1%, whereas the crystallinity increase during heating from 40 to 100 °C is 5.4%, which is smaller. This indicates that during heating, part of the crystals can be melted and recrystallized into more stable lamellar crystals.

Without question, the morphology of PH random copolymer crystallites is kinetically controlled. The process of segmental segregation plays an important role in subsequent growth and perfection of crystals. With the assistance of such a preordering process, the lamellar structure formation is favored at high temperatures. While at low temperatures, the crystallization rate is greatly enhanced. However, once parts of i-PP crystallizable segments are segregated from the amorphous matrix, driven by a large degree of supercooling, they are rapidly crystallized into a less ordered structure. The formed crystals are probably small block-like with no or little correlation with each other.

CONCLUSIONS

The crystallization and melting behavior of isotactic propylene-hexene (PH) copolymer was investigated by using time-resolved SAXS/WAXD technique. Based on the analysis, some relevant conclusions on the morphology, structure and crystallization kinetics can be summarized as follows.

1. The PH random copolymer with 5.7% mole fraction of hexene content can only form α-phase crystal of i-PP homopolymer. The hexene component cannot be incorporated into the unit cell under this concentration.
2. The kinetics of crystallization varies with temperature; and it plays an important role in the development of crystalline structure. At high temperature (e.g., 100 °C), the system exhibits a long induction period, during which segmental segregation between propylene and hexene component (often termed liquid–liquid phase separation) takes place. The segregation can serve as a preordering process and lead to the formation of thermally stable lamellar crystal structure. At low temperature (e.g., 40 °C), the propylene component is rapidly crystallized from the matrix and frozen into small crystal blocks as a result of the low chain mobility and large supercooling.
3. The heating experiments confirmed that the crystallites formed at 40 °C are less stable. Furthermore, upon heating, part of crystal blocks can be melted and recrystallized into more thermally stable lamellar crystals.

The authors thank the assistance of Lixia Rong and Jie Zhu for synchrotron SAXS and WAXD experimental setup. The financial support of this work was provided by the National Science Foundation (DMR-0906512) and ExxonMobil Chemical Company.

REFERENCES AND NOTES

1 De Gennes, P. G. Macromol Symp 2003, 191, 7–10.

2 Fredrickson, G. H.; Milner, S. T.; Leibler, L. Macromolecules 1992, 25, 6341–6354.

3 Semenov, A. N. Phys Rev E 2006, 73, 041803.

4 Semenov, A. N. Eur Phys J B 1999, 10, 497–507.

5 Andrey, V. D. J Chem Phys 1997, 107, 9234–9238.

6 Nesarikar, A.; Olvera De La Cruz, M.; Crist, B. J Chem Phys 1993, 98, 7385–7397.

7 Crist, B. Polymer 2003, 44, 4563–4572.

8 Hanna, S.; Romouribe, A.; Windle, A. H. Nature 1993, 366, 546–549.

9 Crist, B.; Howard, P. R. Macromolecules 1999, 32, 3057–3067.

10 Crist, B.; Mirabella, F. M. J Polym Sci B 1999, 37, 3131–3140.

11 Crist, B.; Finerman, T. M. Polymer 2005, 46, 8745–8751.

12 Silvestre, C.; Cimmino, S.; Triolo, R. J Polym Sci B 2003, 41, 493–500.

13 Wright, K. J.; Lesser, A. J. Macromolecules 2001, 34, 3626–3633.

14 Brandrup, J.; Immergut, E. H.; Grulke, E. A.; Abe, A.; Bloch, D. R. Polymer Handbook, 4th ed.; Wiley: New York, 1999.

15 Poon, B.; Rogunova, M.; Hiltner, A.; Baer, E.; Chum, S. P.; Galeski, A.; Piorkowska, E. Macromolecules 2005, 38, 1232–1243.

16 De Rosa, C.; Delloiacono, S.; Auriemma, F.; Ciaccia, E.; Resconi, L. Macromolecules 2006, 39, 6098–6109.

17 Lotz, B.; Ruan, J.; Thierry, A.; Alfonso, G. C.; Hiltner, A.; Baer, E.; Piorkowska, E.; Galeski, A. Macromolecules 2006, 39, 5777–5781.

18 Glatter, O.; Kratky, O. Small Angle X-Ray Scattering; Academic Press: New York, 1982.

19 Wang, Z. G.; Hsiao, B. S.; Sirota, E. B.; Agarwal, P.; Srinivas, S. Macromolecules 2000, 33, 978–989.

20 Okada, T.; Saito, H.; Inoue, T. Macromolecules 1992, 25, 1908–1911.

21 Pogodina, N. V.; Siddiquee, S. K.; Van Egmond, J. W.; Winter, H. H. Macromolecules 1999, 32, 1167–1174.

22 Iijima, M.; Strobl, G. Macromolecules 2000, 33, 5204–5214.

23 Sung, B. J.; Yethiraj, A. J Chem Phys 2005, 122, 234904.

24 Houdayer, J.; Muller, M. Europhys Lett 2002, 58, 660–665.

25 Hu, W.; Mathot, V. B. F.; Frenkel, D. Macromolecules 2003, 36, 2165–2175.

26 Houdayer, J.; Muller, M. Macromolecules 2004, 37, 4283–4295.

27 Velankar, S.; Cooper, S. L. Macromolecules 2000, 33, 382–394.

28 Wignall, G. D.; Alamo, R. G.; Ritchson, E. J.; Mandelkern, L.; Schwahn, D. Macromolecules 2001, 34, 8160–8165.

29 Li, Y.; Akpalu, Y. A. Macromolecules 2004, 37, 7265–7277.

30 Flory, P. J. Trans Faraday Soc 1955, 51, 848–857.

31 Guinier, A.; Fournet, G. Small-Angle Scattering of X-Rays; Wiley: New York, 1955.

32 Akpalu, Y. A.; Amis, E. J. J Chem Phys 1999, 111, 8686–8695.

33 Akpalu, Y. A.; Amis, E. J. J Chem Phys 2000, 113, 392–403.